Human heart failure biomarker immunosensor based on excessively tilted fiber gratings

BINBIN LUO,[1,2,3,7] SHENGXI WU,[4,*] ZHONGHAO ZHANG,[4] WENGEN ZOU,[1] SHENGHUI SHI,[1] MINGFU ZHAO,[1] NIANBING ZHONG,[1] YONG LIU,[2] XUE ZOU,[1] LINGLING WANG,[4] WEINA CHAI,[5] CHUANMIN HU,[6] AND LIN ZHANG[3]

[1]*Chongqing Key Laboratory of Optical Fiber Sensor and Photoelectric Detection, Chongqing University of Technology, Chongqing, 400054, China*
[2]*School of Opto-electronic Information, University of Electronic Science and Technology of China, Chengdu, 610054, China*
[3]*Aston Institute of Photonic Technologies, Aston University, Birmingham, B4 7ET, UK*
[4]*School of Pharmacy and Bioengineering, Chongqing University of Technology, Chongqing, 400054, China*
[5]*The First Affiliated Hospital of Chongqing Medical University, Chongqing, 400050, China*
[6]*Department of Clinical Biochemistry, Third Military Medical University, Chongqing, 400038, China*
[7]*luobinbin@cqut.edu.cn*
[*]*sxwu2004@cqut.edu.cn*

Abstract: A label-free immunosensor platform based on excessively tilted fiber gratings (Ex-TFGs) was developed for highly specific and fast detection of human N-terminal pro-B-type natriuretic peptide (NT-proBNP), which is considered a powerful biomarker for prognosis and risk stratification of heart failure (HF). High-purity anti-NT-proBNP monoclonal antibodies (MAbs) prepared in our laboratory were immobilized on fiber surface through the staphylococcal protein A (SPA) method for subsequent specific binding of the targeted NT-proBNP. Utilizing fiber optic grating demodulation system (FOGDS), immunoassays were carried out *in vitro* by monitoring the resonance wavelength shift of Ex-TFG biosensor with immobilized anti-NT-proBNP MAbs. Lowest detectable concentration of ~0.5ng/mL for NT-proBNP was obtained, and average sensitivity for NT-proBNP at a concentration range of 0~1.0 ng/mL was approximately 45.967 pm/(ng/mL). Several human serum samples were assessed by the proposed Ex-TFG biomarker sensor, with high specificity for NT-proBNP, indicating potential application in early diagnosing patients with acute HF symptoms.

OCIS codes: (280.1415) Biological sensing and sensors; (060.2370) Fiber optics sensors; (170.0170) Medical optics and biotechnology.

References and links

1. S. K. Arya and S. Bhansali, "Lung cancer and its early detection using biomarker-based biosensors," Chem. Rev. **111**(11), 6783–6809 (2011).
2. J. Wu, Z. Fu, F. Yan, and H. Ju, "Biomedical and clinical applications of immunoassays and immunosensors for tumor markers," TrAC-Trend in Anal.Chem **26**, 679–688 (2007).
3. J. A. Doust, E. Pietrzak, A. Dobson, and P. Glasziou, "How well does B-type natriuretic peptide predict death and cardiac events in patients with heart failure: systematic review," BMJ **330**(7492), 625–632 (2005).
4. S. Li, R. Zhang, P. Li, W. Yi, Z. Zhang, S. Chen, S. Su, L. Zhao, and C. Hu, "Development of a novel method to measure macrophage migration inhibitory factor (MIF) in sera of patients with rheumatoid arthritis by combined electrochemical immunosensor," Int. Immunopharmacol. **8**(6), 859–865 (2008).
5. J. S. Li, Z. S. Wu, H. Wang, G. L. Shen, and R. Yu, "A reusable capacitive immunosensor with a novel immobilization procedure based on 1, 6-hexanedithiol and nano-Au self-assembled layers," Sens. Actuators B Chem. **110**(2), 327–334 (2005).
6. R. Saber, S. Mutlu, and E. Pişkin, "Glow-discharge treated piezoelectric quartz crystals as immunosensors for HSA detection," Biosens. Bioelectron. **17**(9), 727–734 (2002).
7. K. Schmitt, B. Schirmer, C. Hoffmann, A. Brandenburg, and P. Meyrueis, "Interferometric biosensor based on planar optical waveguide sensor chips for label-free detection of surface bound bioreactions," Biosens. Bioelectron. **22**(11), 2591–2597 (2007).

8. K. Qin, S. Hu, S. T. Retterer, I. I. Kravchenko, and S. M. Weiss, "Slow light Mach-Zehnder interferometer as label-free biosensor with scalable sensitivity," Opt. Lett. **41**(4), 753–756 (2016).
9. H. H. Jeong, N. Erdene, J. H. Park, D. H. Jeong, H. Y. Lee, and S. K. Lee, "Real-time label-free immunoassay of interferon-gamma and prostate-specific antigen using a Fiber-Optic Localized Surface Plasmon Resonance sensor," Biosens. Bioelectron. **39**(1), 346–351 (2013).
10. J. Cao, M. H. Tu, T. Sun, and K. T. V. Grattan, "Wavelength-based localized surface Plasmon resonance optical fiber biosensor," Sens. Actuators B Chem. **181**, 611–619 (2013).
11. F. Dell'Olio, D. Conteduca, C. Ciminelli, and M. N. Armenise, "New ultrasensitive resonant photonic platform for label-free biosensing," Opt. Express **23**(22), 28593–28604 (2015).
12. G. Quero, M. Consales, R. Severino, P. Vaiano, A. Boniello, A. Sandomenico, M. Ruvo, A. Borriello, L. Diodato, S. Zuppolini, M. Giordano, I. C. Nettore, C. Mazzarella, A. Colao, P. E. Macchia, F. Santorelli, A. Cutolo, and A. Cusano, "Long period fiber grating nano-optrode for cancer biomarker detection," Biosens. Bioelectron. **80**, 590–600 (2016).
13. K. Zhou, L. Zhang, X. Chen, and I. Bennion, "Optic sensors of high refractive-index responsivity and low thermal cross sensitivity that use fiber Bragg gratings of >80 ° tilted structures," Opt. Lett. **31**(9), 1193–1195 (2006).
14. T. Mueller, A. Gegenhuber, W. Poelz, and M. Haltmayer, "Biochemical diagnosis of impaired left ventricular ejection fraction--comparison of the diagnostic accuracy of brain natriuretic peptide (BNP) and amino terminal proBNP (NT-proBNP)," Clin. Chem. Lab. Med. **42**(2), 159–163 (2004).
15. T. W. Galema, S. C. Yap, M. L. Geleijnse, R. J. van Thiel, J. Lindemans, F. J. ten Cate, J. W. Roos-Hesselink, A. J. Bogers, and M. L. Simoons, "Early detection of left ventricular dysfunction by Doppler tissue imaging and N-terminal pro-B-type natriuretic peptide in patients with symptomatic severe aortic stenosis," J. Am. Soc. Echocardiogr. **21**(3), 257–261 (2008).
16. J. L. Januzzi, Jr., A. A. Chen-Tournoux, and G. Moe, "Amino-terminal pro-B-type natriuretic peptide testing for the diagnosis or exclusion of heart failure in patients with acute symptoms," Am. J. Cardiol. **101**(3 Supplement), 29–38 (2008).
17. L. K. Lewis, S. D. Raudsepp, T. G. Yandle, C. M. Frampton, S. C. Palmer, R. W. Troughton, and A. M. Richards, "Comparison of immunoassays for NTproBNP conducted on three analysis systems: Milliplex, Elecsys and RIA," Clin. Biochem. **46**(4-5), 388–390 (2013).
18. M. Kono, A. Yamauchi, and T. Tsuji, "An immunoradiometric assay for brain natriuretic peptide in human plasmal," Kaku Igaky **13**, 2–7 (1993).
19. P. O. Collinson, S. C. Barnes, D. C. Gaze, G. Galasko, A. Lahiri, and R. Senior, "Analytical performance of the N terminal pro B type natriuretic peptide (NT-proBNP) assay on the Elecsys 1010 and 2010 analysers," Eur. J. Heart Fail. **6**(3), 365–368 (2004).
20. C. Prontera, G. C. Zucchelli, S. Vittorini, S. Storti, M. Emdin, and A. Clerico, "Comparison between analytical performances of polyclonal and monoclonal electrochemiluminescence immunoassays for NT-proBNP," Clin. Chim. Acta **400**(1-2), 70–73 (2009).
21. K. R. Seferian, N. N. Tamm, A. G. Semenov, K. S. Mukharyamova, A. A. Tolstaya, E. V. Koshkina, A. N. Kara, M. I. Krasnoselsky, F. S. Apple, T. V. Esakova, V. L. Filatov, and A. G. Katrukha, "The brain natriuretic peptide (BNP) precursor is the major immunoreactive form of BNP in patients with heart failure," Clin. Chem. **53**(5), 866–873 (2007).
22. Z. Yan, H. Wang, C. Wang, Z. Sun, G. Yin, K. Zhou, Y. Wang, W. Zhao, and L. Zhang, "Theoretical and experimental analysis of excessively tilted fiber gratings," Opt. Express **24**(11), 12107–12115 (2016).
23. B. Luo, Z. Yan, Z. Sun, J. Li, and L. Zhang, "Novel glucose sensor based on enzyme-immobilized 81° tilted fiber grating," Opt. Express **22**(25), 30571–30578 (2014).
24. X. W. Shu, L. Zhang, and I. Bennion, "Sensitivity characteristics of long-period fiber gratings," J. Lightwave Technol. **20**(2), 255–266 (2002).
25. J. Sjöquist, B. Meloun, and H. Hjelm, "Protein A isolated from Staphylococcus aureus after digestion with lysostaphin," Eur. J. Biochem. **29**(3), 572–578 (1972).
26. M. Kangwa, V. Yelemane, A. N. Polat, K. D. Gorrepati, M. Grasselli, and M. Fernández-Lahore, "High-level fed-batch fermentative expression of an engineered Staphylococcal protein A based ligand in E. coli: purification and characterization," AMB Express **5**(1), 70–79 (2015).
27. Z. Yan, Z. Sun, K. Zhou, B. Luo, J. Li, H. Wang, Y. Wang, W. Zhao, and L. Zhang, "Numerical and experimental analysis of sensitivity-enhanced RI sensor based on Ex-TFG in thin cladding Fiber," J. Lightwave Technol. **33**(14), 3023–3027 (2015).

1. Introduction

Immunoassays of protein biomarkers constitute a very powerful tool in the early diagnosis, prognosis, and treatment of serious pathologies such as neurological disorders, cardiovascular diseases and cancer [1–3]. So far, label-free immunosensors based on electrochemical or piezoelectric principles have been widely reported in immunoassays related to pathologies or biomedical research fields [4–6]. Besides, owning to high sensitivity and specificity, compact structure, and capacity of rapid detection, label-free optical immunosensors attract increasing

attention from researchers in recent years. Indeed, many types have been proposed, including optical biosensors based on interferometric strategy [7, 8], surface Plasmon resonance (SPR) based biosensors [9, 10], a planar waveguide ring resonator designed for detecting multiple lung cancer biomarkers [11], and long period fiber grating (LPFG) for differentiated thyroid cancer biomarker detection [12].

In this work, we propose an easily-made and label-free immuno-sensing platform based on excessively tilted fiber gratings (Ex-TFGs) [13] for the specific and fast detection of human heart failure (HF) biomarkers. Human N-terminal pro-B-type natriuretic peptide (NT-proBNP), a non-bioactive fragment containing 76 terminal amino acids, is a very good cardiac biomarker reflecting ventricular volume expansion, pressure overload, and myocardial damage presence and even its degree [14]. Therefore, detecting serum NT-proBNP levels has been approved as an extremely effective method and is widely used in the early diagnosis, prognosis or risk stratification of HF in clinical applications [15]. Indeed, NT-proBNP levels in patients with HF related diseases are overtly increased compared with those of healthy individuals. In general, diagnosis in patients with acute HF symptoms is achieved with fixed cutoff values for NT-proBNP of 0.45 ng/mL and 0.9 ng/mL for ages of <50 and 50~75, respectively [16]. Currently, many methods have been applied for NT-proBNP detection, with each having several disadvantages. For example, radioimmunoassay (RIA) [17] and immunoradiometric assay (IMRA) [18] are complex, time consuming and expensive, and may also cause radioactive contamination. Other methods, such as enzyme linked immunosorbent assay (ELISA) [19], electrochemiluminescence [20], and time-resolved immunofluorescence [21], are commonly used for NT-proBNP quantification, but require large equipment and are less convenient or fast, which makes them unsuitable for emergency and on-site inspections.

The Ex-TFG immuno-sensing platform designed in this study focused on potentially excluding/including acute HF patients through evaluation of NT-proBNP concentrations in human serum in early clinical diagnosis. Ex-TFG based immunosensor development comprised several surface-modified steps, including silanization, adsorption of staphylococcal protein A (SPA), and immobilization of anti-NT-proBNP monoclonal antibodies (MAbs). The most critical step was the immobilization of high-purity anti-NT-proBNP MAbs through the SPA biofilm. Immunoassays, monitoring the specific binding between anti-NT-proBNP MAbs and NT-proBNP, were carried out *in vitro* by monitoring the core-to-cladding mode coupling wavelength shift of Ex-TFG immunosensors.

2. Material and fabrication

2.1 Fabrication of Ex-TFGs and apparatus

Ex-TFGs used as the sensing platform were structured with wide tilted angle (>80°) refractive index fringes inscribed in the core region of SM28 fibers to couple a light portion from the core mode to high-order cladding modes [13]. Using the scanning mask technique and doubled frequency Ar^+ laser emitting at 244 nm with a power level of ~150 mW, a customized amplitude mask (period of 6.6μm) was tilted at 78°. This produced approximately 81° excessively titled fringes with a period along the fiber axis of ~32μm in the core region (See inset of Fig. 1(a)). Such structure can couple the phase-matching light from the core mode to co-propagating high-order cladding modes. The phase matched conditions can be expressed as

$$\lambda_{co-cl} = (n_{co}^{eff} - n_{cl,m}^{eff}) \cdot \Lambda_G / \cos\theta. \tag{1}$$

where λ_{co-cl} is the resonance wavelength, n_{co}^{eff} and $n_{cl,m}^{eff}$ are the effective mode indexes of the fundamental core and m^{th} cladding modes, respectively, Λ_G is the normal period of grating, and θ is the tilt angle of the fringes. Usually, tilt angles of the fabricated Ex-TFGs were from

79° to 83°. The surrounding refractive index (RI) sensitivity of the sensor is affected by a tilt angle increase, but the influence is low in this range [22]. In order to guarantee the cladding-mode resonance to appear in the ~1550 nm wavelength range, 81° tilt angle was selected.

Such Ex-TFGs could be regarded as LPFGs with a much smaller grating period, thus are inherently very sensitive to RI and can be implemented as an optical fiber biosensor platform [13]. RI and temperature properties for Ex-TFGs have been described in previous reports by our group [23]. Due to the highly standardized fabrication process, Ex-TFGs are inexpensive, easily-made and reproducible, unlike interferometer-based or ring-resonator-based biomarker sensors. Therefore, we fabricated several Ex-TFGs with identical parameters for the following experiments.

The experimental apparatus to assess the transmission spectrum is shown in Fig. 1(a). The fiber optic grating demodulation system (FOGDS) (MOI-SM125, accuracy of 1pm) is integrated with a sweep laser light source (1510~1590 nm, 1Hz). Light from one channel (i.e. output channel) of the FOGDS was launched into the SM28 fiber, while the reflected light was isolated by a fiber optic isolator (FOI). A polarizer was used to produce linearly polarized light, whose polarization direction was adjusted by a three ring polarization controller (PC). Transmission spectrum of Ex-TFGs was recorded by another channel (i.e. input channel) of the FOGDS.
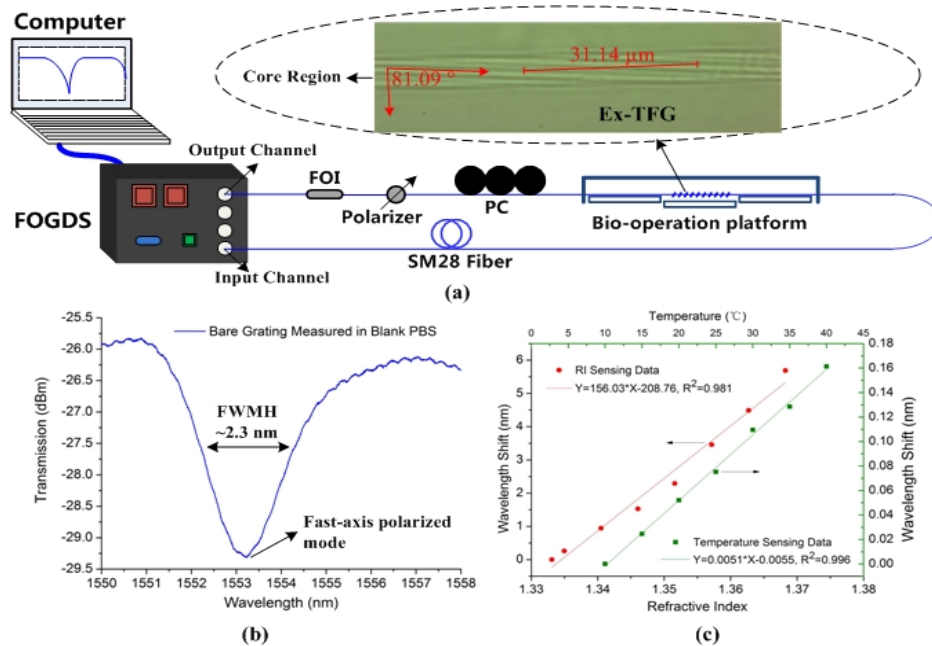

Fig. 1. (a) Experimental setup, Inset: micrograph of the Ex-TFG's core region. (b) Transmission spectrum of a fabricated Ex-TFG with the fast-axis polarized mode at 1550~1558 nm region fully excited, and (c) corresponding RI and temperature properties.

Figure 1(b) shows the transmission spectrum located at the 1550~1558 nm region for one of the fabricated Ex-TFGs with fast-axis polarized mode fully excited, showing that the FWHM (~2.3 nm) is much narrower than that of the conventional LPFG-based or SPR-based strategy (usually >~20 nm and >~50 nm, respectively). Theoretically speaking, measurement accuracy of Ex-TFGs would be much better than that of conventional LPFGs. Furthermore, calibrated results showed that RI and temperature sensitivities of the fabricated Ex-TFGs were 150.0~160.0 nm/RIU and 4.9~5.2 pm/°C, respectively, for each fast-axis polarized mode at the 1550~1558 nm region. Figure 1(c) depicts the sensing properties for the Ex-TFG

resonance spectrum shown in Fig. 1(b), indicating a much higher RI sensitivity but far lower temperature cross-talk effect than values obtained for conventional LPFGs [24].

In a word, although some interferometer-based [7, 8] or ring-resonator-based [11] biosensors exhibit very high RI sensitivity and extremely good Q-factor, their fabrication processes are relatively more complicated, with rigid technical requirements, compared with the proposed Ex-TFG sensors. Meanwhile, SPR-based [9, 10] and conventional LPFG-based [12] biosensors have too wide FWHM, which results in relatively low detection accuracy. Therefore, all the above advantages make Ex-TFGs a favorable platform for biochemical sensing.

2.2 Reagents

3-Aminopropyltriethoxysilane (APTES), highly purified SPA, fluorescein isothiocyanate (FITC), bovine serum albumin (BSA), 1-ethyl-3-[3-dimethylaminopropyl]carbodiimide hydrochloride (EDC), N-Hydroxysuccinimide (NHS), polyethylene glycol (PEG-1500), hypoxanthine-aminopterin-thymidine (HAT) and hypoxanthine-thymidine (HT) supplemented medium were purchased from Sigma-Aldrich, China. Glycine and isopropyl-β-D-thiogalactoside (IPTG) were from Gen-View Scientific, USA. Phosphate buffered solution (PBS) (0.01M, pH7.4) and 4-morpholineethanesulfonic acid hydrate (MES) (0.1M, pH5.5~6.7) buffered solution were obtained from Wuhan Boster Biological Technology, China. Protein A and G chromatography media were from GE, USA. NdeI and XhoI were purchased from TAKARA, Japan. The pET20b empty vector was kindly provided by the Third Military Medical University, China. Standard sample of NT-proBNP (initial concentration of 1.57 mg/mL) was purchased from Chongqing Tansheng Technology (China) and diluted in PBS (0.01M, pH7.4) to different concentration levels of 0.1, 0.5, 1.0, 10, 50, 100, 500 and 1000 ng/mL, for immunoassays.

2.3 Preparation and identification of anti-NT-proBNP MAbs

To prepare highly specific NT-proBNP antibodies, the 24 amino acids at the amino terminus of NT-proBNP were used as target antigen; four target antigen repeats were connected by a flexible amino acid fragment (GGGGS), generating a new peptide with a total of 121 amino acids (target antigen - GGGGS - target antigen - GGGGSGGGGSGGGGS - target antigen - GGGGS - target antigen), termed NT-proBNP T3P × 4. The NT-proBNP T3P × 4 gene was amplified by PCR and cloned into pET20b. After identification by digestion and sequencing, it was named T3P × 4-pET20b (Fig. 2(a) and 2(b)). Then, the T3P × 4-pET20b plasmid was transformed into *E. coli* BL21. The recombinant protein was induced by 0.5 mM IPTG at 28°C for 8 hours, denatured and purified by Ni affinity chromatography, and analyzed by SDS-PAGE. BALB/c mice were immunized four times with the purified NT-proBNP, and spleen cells and SP2/0 cells were fused with PEG-1500 to prepare murine anti-NT-proBNP MAbs. SDS-PAGE (10%) revealed a 12 KD recombinant protein purified from *E. coli* cell lysate (Fig. 2(c)). These results indicated that NT-proBNP was highly expressed in *E. coli* BL21. A hybridoma cell line secreting MAbs, named 5E7, was developed by two subclones. After purification by Protein G affinity chromatography, 12 mg NT-proBNP MAbs with 95.70% purity at a concentration of 1.237 mg/mL were obtained (Fig. 2(d)). The specificity of MAbs was identified by Western-blot (Fig. 2(e)).
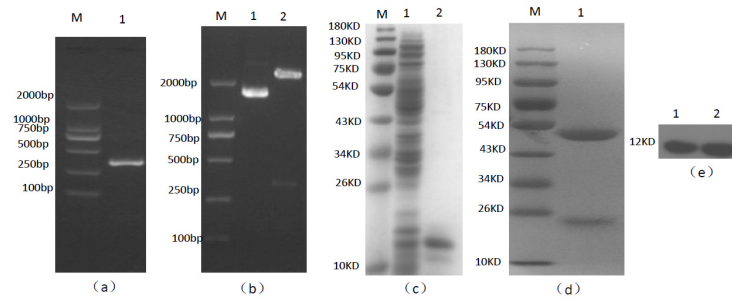
Fig. 2. Preparation and purification of NT-proBNP MAbs. (a) Amplification of the NT-proBNP gene by PCR. Lane 1: PCR product from the NT-proBNP gene. (b) Identification of recombinant vector by restriction endonuclease analysis. Lane 1: T3P × 4-pET20b before digestion; Lane 2: T3P × 4-pET20b digested by NdeI and XhoI. (c) Identification of NT-proBNP by SDS-PAGE. Lane 1: NT-proBNP expressed in *E. coli* transformed with the T3P × 4-pET20b vector induced by IPTG; Lane 2: NT-proBNP purified by Ni affinity chromatography. (d) SDS-PAGE analysis of purified NT-proBNP MAbs from the ascetic fluid. Lane 1: Purified NT-proBNP MAbs. Heavy and light chains are shown. (e) Identification of NT-proBNP MAbs by Western-blot. Lane 1-2: NT-proBNP purified by Protein G affinity chromatography.

2.4 Surface modification of Ex-TFGs

Fabricated Ex-TFGs of identical parameters were initially soaked in the HNO_3 solution (5% v/v) for ~2h at ~40°C, and thoroughly washed with de-ionized water and ethanol. The cleaned Ex-TFGs were immersed in H_2SO_4 (95% v/v in H_2O_2) for ~1h at room temperature to activate the hydroxyl groups on the fiber surface. Then residual liquid droplets were removed using a pipette, before drying in a convection oven for ~6h at ~60°C. Afterwards, the –OH activated Ex-TFGs were immersed in APTES (10%v/v in absolute ethanol) for ~30 min at room temperature, where APTES molecules would bind –OH groups on the fiber surface by silicon-oxygen bonds, as shown in Fig. 3(a). Then, the silanized Ex-TFGs were washed with absolute ethanol and de-ionized water to thoroughly remove non-bound silanized compounds, and dried in convection oven for ~20 min at ~37°C.
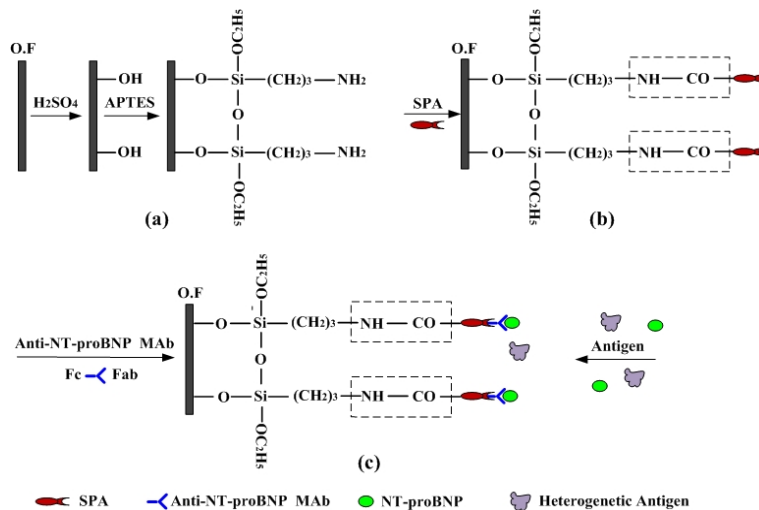

Fig. 3. Chemical bonds of (a) APTES, (b) SPA, and (c) anti-NT-proBNP MAbs on the fiber surface.

SPA, a type I membrane protein extracted from *staphylococcus aureus*, has been shown to bind the immunoglobulin G (IgG) Fc fragment in serum from many mammals without

affecting the bioactivity of the IgG Fab fragment (i. e. the antigen-binding site) while maintaining highly outward-oriented features [25, 26]. Therefore, it has been used as antibody linker for several decades. First, EDC/NHS (0.9 mg/1.2 mg) was added into an SPA solution (0.3 mg/mL in MES buffered solution, pH 6.0, 1 mL) for ~25 min to activate the carboxyl group of SPA. Afterwards, the silanized Ex-TFGs were incubated in the activated SPA solution (300μL, pH 7.2) for ~30 min at room temperature to establish covalent bonds between SPA and APTES (Fig. 3(b)). Then, these sensors were washed with PBS to remove unbound SPA molecules, and air dried. The above process is simple and it need only one time process to active the carboxyl group of SPA for the following immobilization of anti-NT-proBNP MAbs.

Finally, the SPA-modified Ex-TFGs were separated into two groups, labeled 'S1' and 'S2', respectively. Immobilization of anti-NT-proBNP MAbs to the fiber surface was performed by incubating 'S1'and 'S2' Ex-TFGs with the high-purity anti-NT-proBNP MAbs solution (in PBS, phase volume 180μL) at a concentration of 0.30 mg/mL and 0.15 mg/mL, respectively, for ~40 min at room temperature. Then, the functionalized Ex-TFGs were washed several times with PBS to remove unbound anti-NT-proBNP MAbs. Chemical bonds with anti-NT-proBNP MAbs on the fiber surface are described in Fig. 3(c).

3. Results and discussion

3.1 Surface modification monitored by resonance spectra of Ex-TFGs

Using the experimental setup in Fig. 1(a), spectra of the Ex-TFGs immersed in blank PBS (0.01M, pH7.4) were recorded after each step of surface modification. Figure 4(a) represents the spectrum evolution for one of the Ex-TFGs; Fig. 4(b) is the corresponding wavelength shift, indicating that due to the adsorption of APTES, SPA, and anti-NT-proBNP MAb layers, resonance wavelength shifted by ~0.465 nm, ~0.705 nm and ~1.01 nm, respectively, compared with that (~1553.300 nm) of the bare Ex-TFG. Other fabricated Ex-TFGs underwent similar spectrum evolution. This outcome was expected because an increase of outer layer thickness leads to an increase in the surrounding RI. Therefore, as additional layers are immobilized on the fiber surface, resonance wavelengths of Ex-TFGs would red-shift due to the RI sensitivity of the sensor showing a positive value. However, because APTES, SPA and anti-NT-proBNP MAb layers are so thin that the change in the surrounding RI is very small, only a small wavelength shift was obtained.
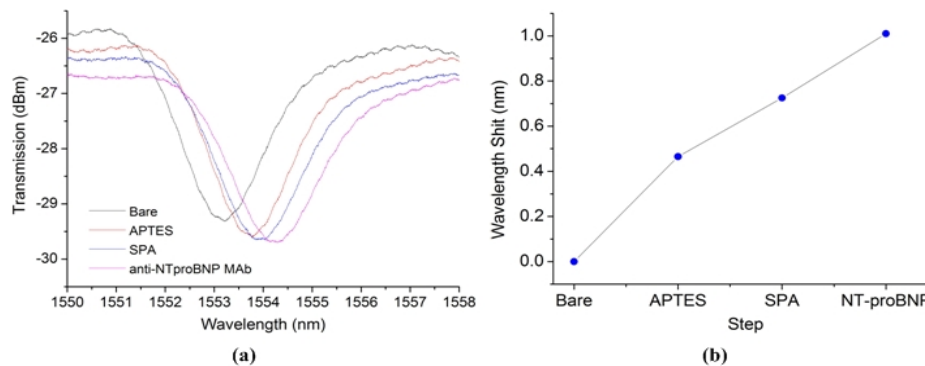

Fig. 4. (a) Spectrum evolution for an Ex-TFG and (b) the corresponding wavelength shift in every step of the surface modification.

3.2 Surface characteristics of modified Ex-TFGs

Uniformity of the APTES and SPA layer on the fiber surface was assessed by scanning electron microscopy (SEM, JSM-6460LV). Surface morphology of the bare, silanized, and SPA-modified fibers are shown in Fig. 5(a), 5(b) and 5(c), respectively. The surface of the

bare fiber was glossy, but became plicate after modification by APTES and SPA. Consequently, the methodology used for silanization and the subsequent SPA modification produced nicely adherent layers on the fiber surface.

However, as shown in Fig. 5(b) and 5(c), there were no overt differences between silanized and SPA-modified fibers; thus, to provide a visual evidence for the SPA layer adhering on the fiber surface, several bare fibers were submitted to the same modification process described in Section 2.4. For one of them, a prepared FITC-labeled SPA solution also activated by EDC and NHS chemistry was used, to modify its surface after APTES treatment. After many washes with PBS, the FITC-labeled-SPA modified fiber was inspected by inverted fluorescence microscopy (Olympus Venox). As shown in Fig. 5(d), strong glowing fluorescence appeared, providing fairly good evidence of a consistent SPA layer established on the fiber surface. However, no fluorescence was observed for APTES-treated fibers (without FITC-labeled-SPA treatment). Therefore, this fluorescence can be attributed to the presence of SPA molecules bound on the fiber surface.
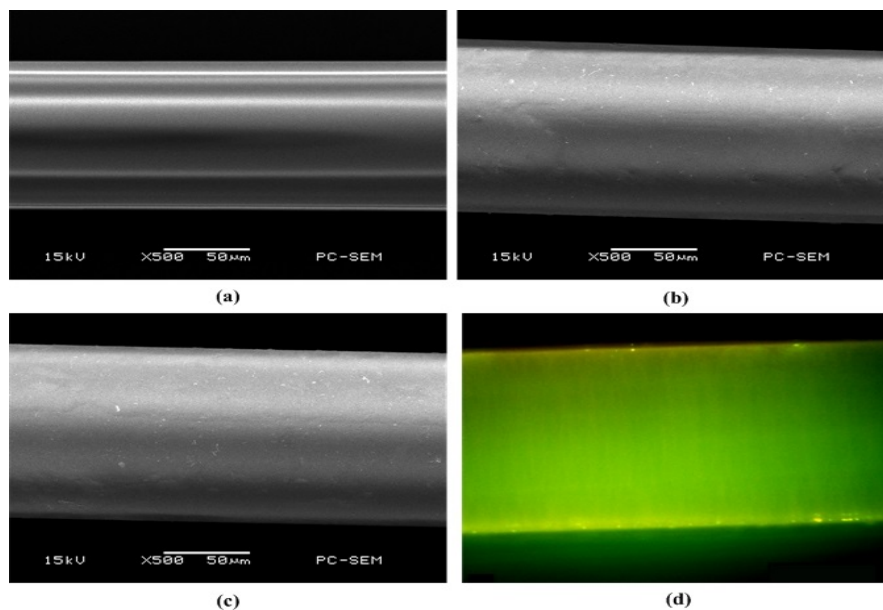

Fig. 5. Micrographs for surface morphology of (a) bare, (b) silanized, and (c) SPA-modified fibers, observed by SEM. (d) Fluorescent micrograph of the FITC-labeled-SPA modified fiber obtained by inverted fluorescence microscopy.

3.3 NT-proBNP detection using Ex-TFG based immunosensors

As shown in Fig. 1(a), the ends of the Ex-TFG immunosensor are fixed on two separated glass slides with a movable slide between them; meanwhile, the body of the sensor is on the middle slide's surface. First, a reference spectrum was recorded after introducing a blank PBS (0.01M, pH7.4) to cover the whole sensor. Subsequently, the prepared NT-proBNP sample solutions with different concentration levels (phase volume of 200μL) were analyzed by the immunosensor in turn, with the sensing region sealed with a small vessel to prevent sample evaporation during the immunoassay. For each concentration, it would take 2~3 min for the sensor to obtain a stable resonance wavelength, which signified a complete specific binding reaction between the anti-NT-proBNP MAbs and NT-proBNP antigens near the fiber surface. Then, the sensor was washed several times with blank PBS before assaying the next concentration level.

Resonance spectra of the Ex-FBGs would red-shift with increased NT-proBNP concentration. Figure 6(a) represents the spectrum evolution for one of the immunosensors,

with overt redshift. This is reasonable because the RI sensitivities of Ex-TFGs are positive, and effective RI values for cladding modes are affected by the specific binding between NT-proBNP antigens and anti-NT-proBNP MAbs.

For the first group of Ex-TFGs ('S1'), average wavelength shifts for all concentration levels are shown in Fig. 6(b) (Blue circle). The above immunoassays were also carried out under the same conditions in the second group of Ex-TFGs ('S2'), whose average wavelengths varied with the NT-proBNP level as shown in Fig. 6(b) (Red Cross). The two groups of immunosensors did not overtly respond until NT-proBNP concentration was ≥0.5 ng/mL; thus, the lowest detectable concentration was estimated at ~0.5 ng/mL. Moreover, the inset in Fig. 6(b) showed that the average wavelength shifts for 'S1' were between ~25 and ~45pm at NT-proBNP concentrations of 0.5 and 1.0 ng/mL, respectively, and were nearly identical to those (i.e. ~20 pm and ~45 pm, respectively) of the second group ('S2'). Average sensitivity for NT-proBNP detection at concentrations ranging from 0 to 1.0 ng/mL was ~45.967 pm/(ng/mL) with an R^2 of ~0.997 by linear fitting [inset of Fig. 6(b)]. Although the immunosensor established in this study is not as sensitive as ELISA [19], it can be operated more easily and quickly, with more consistent results, and no expensive reagents or equipment required.
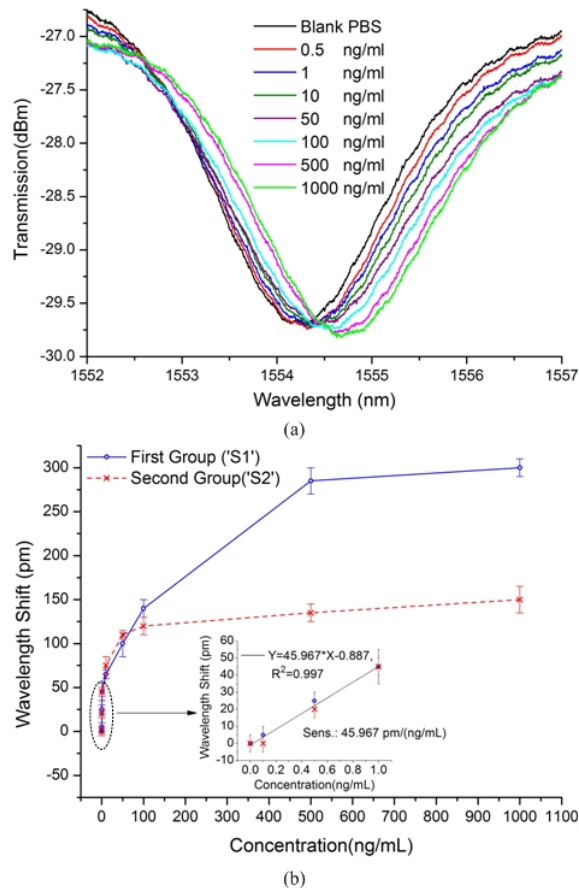

Fig. 6. (a) Spectrum evolution for one of the Ex-TFG immunosensors as NT-proBNP levels change from 0~1000 ng/mL. (b) Average wavelength shifts for the first ('S1') and second ('S2') groups of Ex-TFGs. Relative standard deviation (RSD) from several independent measurements: 0.032 < RSD < 0.222 for 'S1' and 0.045 < RSD < 0.250 for 'S2'; Inset: Magnified picture at the concentration range of 0~1.0 ng/mL.

The inset of Fig. 6(b) shows that the linear dynamic range of the sensor was small, only 0~1.0 ng/ml. This is due to an active length of the sensor of only ~15 mm; thus, the amounts of anti-NT-proBNP MAbs immobilized on the fiber surface are not more than enough, leading to the quantity of NT-proBNP molecules absorbed by the anti-NT-proBNP MAbs being relatively low. Therefore, theoretically speaking, the linear dynamic range of the sensor could be increased by fabricating a longer Ex-TFG immunosensor.

Besides, according to Fig. 6(b), the redshift of the resonance wavelength became saturated gradually; this was due to available Fab antigen binding fragments of anti-NT-proBNP MAbs gradually being decreased with increasing test number. However, the average saturation point (~500 ng/mL) of the first group of Ex-TFGs ('S1') was far higher than that (~100 ng/mL) of the second group ('S2'), which might be attributed to the concentration (0.30 mg/mL) of anti-NT-proBNP MAbs used in the immobilization step for 'S1' being two times that of the second group (0.15 mg/mL), thus leading to a large difference in available anti-NT-proBNP MAbs immobilized on the fiber surface. This corroborates the findings of average wavelength shift (~285 pm) of the first group being ~2.4 times greater than that (~120pm) of the second group at saturation points, i.e. ~500 ng/mL and ~100 ng/mL, respectively.

3.4 NT-proBNP detection in human serum samples

With the concept that sectional fixed values for NT-proBNP levels are 0.45 ng/mL (for <50 years old patients) or 0.9 ng/mL (for 50~75 years old patients) in excluding patients with acute HF symptoms [16], the potential application in the clinic of the current sensing platform was investigated. As shown in the inset of Fig. 6(b), the wavelength shift of calibrated Ex-TFG immunosensors for NT-proBNP levels in serum from acute HF patients was estimated at >20 pm (<50 years old patients) or >45 pm (50~75 years old patients).

Human serum samples with known NT-proBNP levels (2 acute HF patients and 2 healthy volunteers) were obtained from the First Affiliated Hospital of Chongqing Medical University (CQMU), Chongqing, China, and kept at −80°C until analysis. The study protocol was approved by the ethics committee of the First Affiliated Hospital of CQMU, and informed consent was obtained from each subject. An unused Ex-TFG immunosensor of the first group ('S1') was initially immersed in a blank PBS and the observed resonance wavelength was recorded as the reference. Each serum sample was analyzed for ~3 min by this calibrated Ex-TFG immunosensor in turn. After each immunoassay, the sensor was washed with blank PBS several times; resonance spectra were recorded under identical conditions. Wavelength shifts obtained with this immunosensor for serum samples are listed in Table 1, indicating good consistency with early diagnosis results of the hospital. Therefore, the immunosensor worked effectively in excluding or including acute HF. Since that analyses were carried out with clinical serum samples, and given that other types of non-specific antigens exist in this complex environment, the above results revealed a high specificity of the proposed immunosensors for NT-proBNP.

Table 1. NT-proBNP Level in Serum Samples Analyzed by an Ex-TFG Immunosensor ('S1')

Sample	Age	NT-proBNP Level (ng/mL)	Diagnosis by hospital	Wavelength shift (pm)	Result
1	40	0.08	health	± 5.0	Exclude
2	64	0.13	health	5.0 ± 5.0	Exclude
3	48	0.76	acute left HF	30.0 ± 5.0	Not exclude
4	73	1.57	acute left HF	65.0 ± 10.0	Not exclude

Furthermore, NT-proBNP detection in serum samples was also performed with an unused Ex-TFG immunosensor of the second group ('S2'), but consistency with previously calibrated data (inset of Fig. 6(b), Red Cross) was not good, that is, wavelength shifts at similar NT-proBNP levels were overtly larger than those evaluated by the calibration data. This might be

due to many free SPA molecules still not binding anti-NT-proBNP MAbs as a consequence of the low concentration (0.15 mg/mL) of anti-NT-proBNP MAbs used in the immobilization step. Such MAb level might have been insufficient, leading to free SPA molecules that could easily bind other types of antibodies in the sophisticated environment of a real serum sample. On the other hand, these findings suggested that anti-NT-proBNP MAbs used at ~0.3 mg/mL in the immobilization step as in 'S1', could bind all SPA molecules absorbed on the fiber surface.

It should be noted that the above experiments were designed for analyzing NT-proBNP under certain test conditions (active length of Ex-TFGs = 15 mm; SPA solution = 0.3 mg/mL; anti-NT-proBNP MAb solution = 0.3 mg/mL; phase volume of the NT-proBNP solution = 200μL). However, these parameters are selectable according to specific requirements. In such a case, system calibration should be performed anew.

4. Conclusions

We presented an easily-made and label-free immunosensor based on Ex-TFG for the highly specific and fast detection of the human HF biomarker NT-proBNP. Lowest detectable concentration of ~0.5 ng/mL for NT-proBNP was obtained, with average sensitivity for NT-proBNP detection in the concentration range of 0~1.0 ng/mL of ~45.967 pm/(ng/mL). Human NT-proBNP levels in serum from a few clinical samples were detected, demonstrating that the Ex-TFG biomarker sensor for excluding/including acute HF is feasible and could be used in the early clinical diagnosis. The basic concept of the developed device can be easily expanded to obtain label-free biosensors for a wide range of protein biomarkers. Considering that a more precise and sensitive detection of NT-proBNP in human serum is required for diagnosis, prognosis or risk stratification of HF in clinical applications [15], further research will focus on improving the minimum detection limit and sensitivity of the proposed label-free biomarker sensor; this could be realized by using Ex-TFGs inscribed in thin-core-cladding fibers (SM1500) as bio-sensing platforms [27].

Acknowledgments